International Journal of Religion
2024
Volume: 5| Number 7 | pp. 490 – 500
ISSN: 2633-352X (Print) | ISSN: 2633-3538 (Online)
ijor.co.uk
DOI: https://doi.org/10.61707/01g4y035

Unveiling Urban Evolution: Assessing Patterns of Transformation in Guangzhou's Net Production

Hong Li[1]

Abstract

Urban evolution refers to the continuous changes and adaptation of urban environments to social, economic, technical, and environmental changes, acknowledging that cities are dynamic systems. Urbanization and land use/cover change (LULCC), which are mostly caused by human activity, which have a big impact on the environment. These two variables also affect urban vegetation when combined with climate change. We choose Guangzhou City to examine how urban growth processes and spatial changes in urban areas affect net production (NP). A Machine learning [ML] approach such as Support Vector Machine (SVM) was utilized to examine the relationship between NP and urbanization intensity. This study examined to analyze urban evolution, focusing on the patterns of change in the NP in Guangzhou City, China. The findings demonstrated between 2011 and 2023, the NP in the studied region decreased overall and had distinct geographic variation. The mean Urban Development Index (UDI) in Guangzhou increased significantly between 2011 and 2023. In both years, metropolitan exurbs constituted the majority of the urban geographic category, but the most notable increase in urban fringe areas, which accounted for about 2,320.24 km2 of the urban exurbs. Regarding UDI and NP, there was an opposite relationship, suggesting that the growing intensity of the growth of urban expansion negatively affected NP. Urban development intensity negatively influenced NP, with urban fringes experiencing the most significant losses due to an increase in urbanization and a decrease in agriculture.

Keywords: *Urbanization, Net Production (NP), Urban Evolution, Guangzhou, Support Vector Machine (SVM).*

INTRODUCTION

To expand the economies and accommodate a growing population, emerging countries need to regulate the intensity of urban land use while overcoming the obstacles brought by a scarcity of land. The goal of Chinese study is to balance social, environmental, and economic variables in urban environments while optimizing outputs.

Understanding Urban Land-Use Intensity in Emerging Nations: The demand for urban land in emerging nations continues to escalate due to advancing economic development and population growth. To address the challenge, there are two primary approaches: densification of land use and increased urbanization [1]. However, limitations on available land hinder cities from expanding extensively, despite the potential for heightened land-use intensity through concentrated usage. Land utilization concentration is a notion that has its roots in the agricultural sector, and remains relevant and applicable in contemporary urban contexts [2].

Exploring the Origins and Applications of Land-Use Intensity: The extent to which sociopolitical inputs like labor, assets, fuel, water and funding or human activities themselves, increase agricultural output is known as the intensity of land use in the field of farming. The enhancement stems from the adoption of advanced technologies and management practices [2]. While the notion of the magnitude associated with urban development is less well-defined, Chinese researchers have extensively studied and conceptualized and compared to their counterparts [3]. It perceives urban land use not simply as intensifying input on land but as a strategic increase aimed at maximizing output. The intricacies and distribution of land use in urban areas are intricately linked to land-use intensity, reflecting the complexities of urban land utilization [4].

Defining Urban Land Use Intensity-A Multi-dimensional Perspective: The frequency of land usage encompasses the amplified output and its implications on the economy, environment, and society. It is defined reflects the level of production enhancement resulting from improved finest land utilization combinations and administration techniques in an urban area, considering the prevailing situations concerning the intersection of

[1] International College, Krirk University,Bangkok,10220,Thailand, E-mail: lehon_1234@126.com

technology and economy [5]. Crucially,the entirety of a city's borders remains constant, highlighting the importance of achieving enhanced production while considering social, environmental, and economic consequences [6].

Aim of the study: The study focuses on the impact of urban growth and spatial variations on NP in Guangzhou City, China, using the support vector machine (SVM)in UDI to examine the relationship between NP and urbanization intensity.

LITERATURE REVIEW

The literature discusses Guangzhou's urban development, incorporating cultural sustainability analysis, Evolutionary Game Theory, empirical NP studies, and addressing challenges and opportunities for sustainable urban development.

Historical Context of Urban Development in Guangzhou: To complement the current typo-morphological approach [7] integrated the viewpoint of societal viability study using standard typo morphological urban spatial analysis techniques. The perspective aims to direct the evolution of urban morphology through cultural sustainability frameworks. However, the institutionalization analysis reveals gaps in public engagement in China's urban regeneration [7]. Additionally the authorof [8] delves into the underlying logic shaping metropolitan nighttime ecosystems, using four bar streets in Guangzhou, China, as a case study.

Theoretical Frameworks for Understanding Urban Evolution: An Evolutionary Game Theory (EGT) in road transportation networks [9] outlines its applications in traffic management, behavioral interactions, routing operations, choice-based analysis, and transport safety. Furthermore, according to the study [10] presented an embedding-driven clustering approach, using Singapore as a case study, to understand the spatiotemporal evolution of urban landscapes. Work of [11] suggested three approaches to mid-level conceptualization based on urban China cases, offering new analytical frameworks for urban studies.

Empirical Studies on Guangzhou's Net Production (NP): Investigating green economic growth and green total factor productivity (GTFP) [12] researchers used panel data from Chinese cities to analyze the impact of the digital economy. Author of [13] introduced a static-dynamic intuitionist fuzzy assessment framework for sustainable development, emphasizing real interactions and policy implications. Study by [14] examined the daily urban activity failures in Guangzhou, utilizing both quantitative and qualitative data from 2021 fieldwork.

Challenges and Opportunities for Sustainable Urban Development: Examining AI's role in urban planning [15] researchers explore how AI technologies support intelligent and sustainable development. Considering global socio-ecological concerns [16] emphasized the necessity of sustainable population and resource consumption scenarios. Furthermore study [17] suggested the importance of maintaining natural and agricultural land per person for ecosystem sustainability and human well-being. Through case studies and a variety of techniques, the merging of eco-cities, data-driven smart cities, and ecologically data-driven smart sustainable cities paradigms offers an integrated model [18] for strategically sustainable urban growth.

MATERIALS AND METHODS

The study used a comprehensive methodology, including data gathering and preprocessing using MOD17A3 NP product data, Landsat TM images, and meteorological data. The classification of LULCC was done using the Spectral Angle Mapper classifier, while the CASA model was used to estimate NP. Trend analysis was done using Mann-Kendall and Theil-Sen median slope estimators. The impact of human-driven LULCC on NP was assessed using the relative impact indicator. The UDI was created using SVM methodology to quantify urbanization levels based on land cover change, economic activity, and demography.

Experimental Design

Guangzhou City, an urban area of 7434.4 km^2 with 9 districts, is situated in the south-central region of Guangdong Province. Plains and steep areas make up its landscape, and the average annual temperature varies from 21.4 to 21.9 °C. Additionally, 1689.3 to 19882.7 mm of precipitation fell on it. The city expanded quickly Regarding the Chinese late 1970s financial liberalization and reforms and well-executed strategic urban master

planning plans. With a population of around 12.9 million, the region's GDP increased from $268.48 billion in 2011 to $1,542.01 billion in 2023. Urban development laws, population growth and economic development have contributed to the rapid expansion of cities and changes in land cover in **Figure 1.**

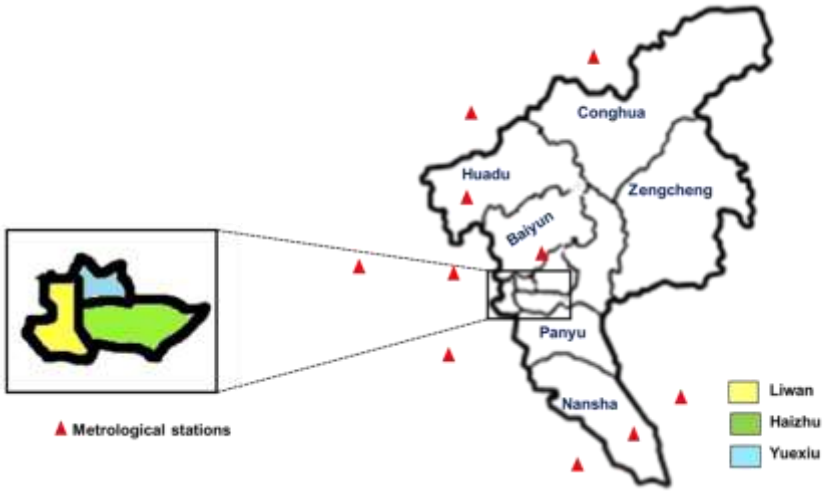

Figure 1. Study area.

Data gathering and Preprocessing

This study used multiple datasets for data collection and preprocessing. The first dataset was Moderate Resolution Imaging Spectroradiometer (MODIS) Version 17A3 (MOD17A3) NP product data from Guangzhou, which was converted using the MODIS Reprojection Tool. The second dataset was land use/cover change information from Landsat TM images, corrected with FLAASH. The third dataset was meteorological data from 13 climatological stations, interpolated using Kriging.

MOD17A3 NP Product and Uncertainty: MOD17A3 throughout NP product data from Guangzhou, which is accessible from the Terrestrial Observation and Prediction System (TOPS) is used in the study for the years 2011 to 2018. Using the MODIS Reprojection Tool, prepared Hierarchical Data Format Earth Observing System (HDF EOS) files are converted to the Albers Conical Equal Area projection. Daily data on the weather, Fraction of Photosynthetically Active Radiation(FPAR) and Leaf Area Index(LAI) things, and MODIS surface area goods are the three sources of input for each pixel. Because of errors across related classes, the accuracies of the MOD12Q1 and MOD15A2 datasets fall between 70% and 80%. These datasets are higher quality to techniques like temporal filling and non-linear spatial interpolation. With a low relative error in the calculation of rice yield and great consistency when compared to field data, field measurements have shown the uncertainties associated with MOD17 products.

Land use/cover change (LULCC) from Landsat Thematic Mapper (TM): Land cover and usage in Guangzhou were determined using a collection of multispectral Landsat TM images captured in 2011, 2023, and 2022. Using these images, which have a thirty-meter distance and seven wavelengths that range from the vision to the infrared spectrum, land cover information was collected for classification samples. Additionally, four multispectral bands and a 2.5-m panchromatic band were recorded for a SPOT picture in December 2016. Speed in Path of Sight Using the Atmospheric Analysis of Spectral Hypercube atmospheric calibration approach, sensor radiance was adjusted for atmospheric impacts.

Atmospheric Data: The meteorological dataset to look into the influence on NP variability extends the years 2014–2022 and contains information on the monthly mean temperature and the total amount of precipitation that falls in the greater Guangzhou area of each month. In particular, 13 climatological stations' historical monthly temperature and precipitation records were obtainedfrom the appropriate Statistical Annual and the

Guangzhou Economic Data website. Kriging is a significant interpolation technique that is frequently used to sample the climatic parameters from the site-based data at each pixel.

Land Use/ Cover Change (LULCC) Classification

Target discrimination can be achieved using the Spectral Angle Mapper (SAM) classifier in n-dimensional space. A threshold is set when there is a wavelength slope fewer than the limit between the object of interest and benchmark components. SAM, when combined with vegetation distribution criteria, can improve classification accuracy for six forest-woodland-savannah mosaic species by 10% by eliminating the effects of vegetation and environmental background.In Guangzhou, China, the Spectral Angle Mapper. Table 1 displays the five plant kinds that have been selected from the Geosphere-Biosphere Program (GBP) schemes based on the current land covers in Guangzhou.

Table 1. GBP definitions and criteria used for the LULCC classes.

Types of LULCC	Canopy Cover (%)	Canopy Woodland Environments	Description
Evergreen Broadleaf Forests (EBF)	>60	Green Comprehensive leaf forest species	Territories mostly covered by broadleaf trees that are taller than two meters and have a canopy cover of more than 60%. Nearly all trees have year-round greenery.
Mixed Forests (MF)	>60	A combination of different kinds of forests, but any covering that is over sixty percent	Areas covered in forests of evergreen broadleaf and needle leaf.
Evergreen Needle leaf Forests (ENF)	>60	Green Needle leaf forest species	Regions are mostly covered by plants via an overhang of needle leaves of greater than 60 percent and heights beyond two meters. Nearly every tree is evergreen throughout the year.
(Open) Shrub lands (SL)	10–60	Woody plants are often shrubs, that are under two meters in height	Regions with woody vegetation that is less than two meters tall and primarily covered in shrubs, and regions with herbaceous cover where shrubs make up more than 60% of the vegetation
Woody Savannas (WS)	30–60	Herbaceous and other understory systems	Areas where there are between 10% and 30% of trees and grassy vegetation.

Estimating NP using the Carnegie-Ames-Stanford Approach (CASA)

The light usage efficiency-based parameter-based CASA model was used to evaluate NP. Calculating the CASA model involves multiplying the actual light consumption efficiency (ε) ($gC \cdot MJ \cdot m^{-1}$) by the quantity of received photosynthesis energetic radiation ($MJ \cdot m^{-2}$). The expression for NP is (Equation 1):

$$NPP(w,s) = APAR \times \varepsilon \qquad (1)$$

Where$NPP(w,s)$ ($gC \cdot MJ \cdot m^{-2}$) is the NP for grid cell w in month$s$. Equation (2)can be used to calculate the real light utilization efficiency (ε) that is dependent on the temperature and water level.

$$\varepsilon(w,s) = S_1(w,s) \times S_2(w,s) \times X(w,s) \times \varepsilon_{max} \qquad (2)$$

Where $X(w,s)$ is a moisture stress coefficient, $S_1(w,s)$ and $S_2(w,s)$ are temperature stress coefficients, and ε_{max} is the highest light utilization efficiency that needs to be simulated for each plant species. The conditions that affect ε_{max} can vary greatly and mostly determined by the type of soil, temperature, and water availability.$FPAR$is dependent upon solar surface energy ($MJ \cdot m^{-2}$) whereas PARis calculated as the sum of PAR and the percentage of energy through photosynthesis productive. Consequently, NPP at location w and time s becomes (Equation 3):

$$NPP(w,s) = FPAR \times SOL \times 0.5 \times S_1(w,s) \times S_2(w,s) \times X(w,s) \times \varepsilon_{max} \qquad (3)$$

Equation (4) defines$FPAR$as an expression of the simple ratio (SR) and the $NDVI$:

$$FPAR(w,s) = \alpha FPAR_{NDVI} + (1-\alpha) FPAR_{SR} FPAR \in [0.001, 0.95] \qquad (4)$$

Whereα is set to 0.5,According to Equation (5), the NDVI-FPAR approach and Equation (6) SR-FPAR model, respectively, yield the following FPAR values: $\alpha FPAR_{NDVI}$ and $FPAR_{SR}$.

$$FPAR(w,s) = \frac{(NDVI(w,s)-NDVI_{j,min})\times(FPAR_{max}-FPAR_{min})}{(NDVI_{j,max}-NDVI_{j,min})} + FPAR_{min} \quad (5)$$

$$FPAR(w,s) = \frac{(SR(w,s)-SR_{j,min})\times(FPAR_{max}-FPAR_{min})}{(SR_{j,max}-SR_{j,min})} + FPAR_{min} \quad (6)$$

Where$NDVI_{j,max}$, and $NDVI_{j,min}$values represent 95% and 5% of the population that is covered through the NDVI, correspondingly and j; $SR_{j,max}$, and $SR_{j,min}$resemble$NDVI_{j,max}$, and$NDVI_{j,}min, NDVIi$, min accordingly. Thus, we can use (Equation (7)) to explain the relationship between $NDVI$and SR:

$$SR(w,s) = \left[\frac{1+NDVI(w,s)}{1-NDVI(w,s)}\right] \quad (7)$$

$$X(w,s) = 0.5 + 0.5 \times FS(w,s)/OFS(w,s) \quad (8)$$

The impact of the seedlings' actual water conditions is shown by the moisture stress coefficient (W), it's capable to determine the amount of light consumed. It is calculated using the regional actual evapo-transpiration (ET) (mm) and projected, which are originating via MOD16A2 items.

Theil–Sen Median Slope Estimator and Mann-Kendall (M-K) Trend Analysis

This study utilizes a reliable non-parametric M-K technique, employed for long-term trend analysis of abnormal data, to examine both the geographical and temporal NP change trends. According to reports, the sample size $n \geq 8$ corresponds to an essentially distributed Y for the M-K test statistic. A monotonic pattern of growing or decreasing might be shown by a positive or negative Y value. Equation (9) is used to obtain the M-K test statistic T.

$$T = \sum_{j=1}^{m-1}\sum_{j=1+1}^{m} sgn(w_i - w_j) \quad (9)$$

wherew_i and $w_j$are the data values in time series j and $i(i > j)$, respectively; n is the number of data points; and $sgn(w_i - w_j)$ is the sine function, which is represented by Equation (10):

$$sgn(w_i - w_j) = \begin{cases} 1, if w_i - w_j > 0 \\ 0, if w_i - w_j = 0 \\ -1, if w_i - w_j < 0 \end{cases} \quad (10)$$

Equation (11) is used to compute the variance.

$$Var(T) = \frac{m(m-1)(2m+5)-\sum_{j=1}^{n} s_j(s_j-1)(2s_j+5)}{18} \quad (11)$$

Where$N$ the amount of connected collections,s_j is the quantity of length connections$i$, and m is the number of data points. A gathering of sample term for identically valued information is a linked cluster. In cases when population sample size exceeds eight, the conventional normal test statistic is used (Equation (11)) and is calculated using Equation (12).

$$Y = \begin{cases} \frac{t-1}{\sqrt{Var(T)}}, if T > 0 \\ 0, if T = 0 \\ \frac{t+1}{\sqrt{Var(T)}}, if T < 0 \end{cases} \quad (12)$$

In this study's significance tests over time, $theY$ score threshold of the five percent threshold for significance is 1.96, while the one percent substantial level is 2.576 was used to assess the significance and trend direction.The Theil–Sen median slope estimator can be created using the following formula, it can be used to

calculate the frequency of variation in a brief or chaotic time series and for calculating the trajectory's gradient in an example in M data set pairs:

$$\beta_j = Median\left(\frac{w_i - w_l}{i-l}\right) for j = 1,..,M \qquad (13)$$

When the data values at periods i and l ($i > l$) are represented by the variables $w_i$and w_l.

Impacts of Weather and LULCC Variations on NP

We assessed the impact of human-driven LULCC on NPP using the relative impact indicator (RII). To calculateRII, NPP_{lulcc} and NPP_Owere utilized, namely in Equation(21):

$$RII = \frac{NP_{kvkdd}}{NP_O} \times 100\% = = \frac{NP_O - NP_{lulcc}}{NP_O} \times 100\% \qquad (14)$$

NP_O represents the NP of prospective vegetation, whereas NP_{lulcc} represents the NP variability caused by $LULCC$ because of human activity. If$RII > 0$, it suggests that LULCC is having a detrimental influence on NP and vegetation activity; if $RII <$0, it suggests either human impact is minimal or that vegetation management and protection are more successful.It suggests that when $|RII|$more than 50%, $LULCC$ is the main cause of the shift inNP. Togain further knowledge on RII and the NP_O computation.

The Relative Effects of LULCC and Climate Change on NP

Equation (22) represents the relationship that exists between yearly NP and meteorological variables like precipitation, solar radiation, and temperature).

$$Q_{wz} = \frac{\sum_{j=1}^{m}[(w_j - \bar{w})(z_j - \bar{z})]}{\sqrt{\sum_{j=1}^{m}[(w_j - \bar{w})^2} \times \sum_{j=1}^{m}[(z_j - \bar{z})^2} \qquad (15)$$

Where are the climatic variables and NP mean values from 2011 to 2023, is the correlation coefficient between $w$and z, additionally, w_j and z_j represent the values of NP and climate variables in the i^{th} year, respectively.

$$Contr_{inter} = 100 - Contr_{cli} - Contr_{LULCC} \qquad (16)$$

The overall geographical effects of LULCC and warming temperatures on NP were evaluated by applying an approach, which uses the varied gradient of NP in several situations to measure and contrast the overall effects. The relationship between LULCC and climate change and NPcan be expressed as $\Delta LULCC$ and $\Delta Cli.NPP = Q - Q1$.Considering that, under the scenarios of constant temperature and variable LULCC, accordingly, the angle of NP equaled Q1 and Q2,$NP = Q1 - Q2$, since the slope of real NP was Q. Additional factors influencing NP included $Contr_{inter}.NP = (Q1 + Q2)$-$Q$. Thus, it can be possible to explain how LULCC and NP changes are impacted by changes in the climate and other things.The impacts of LULCC, global warming, and additional factors added together and do not affect a shift in NP. Using a Maxwell Triangle, the three pictures can used to create the synthesized impact image. At the pixel level, the three effect variables' inputs can independently represented.

Urban Development Index (UDI) using Support Vector Machine (SVM)

To quantify the degree of urbanization as it relates to land cover change, economic activity, and demography, we developed the following index: the UDI. The UDI, land cover and change economic activity. To compute UDI, we used data on demographics, economy, and terrain volatility together with an ML method based on SVMs.The types and characteristics of land cover have an impact on the condition regarding land usage of both countryside and urban regions. Because their landscape patches are monotonous, Environmental ordering is greater and volatility is lower in pure rural and urban contexts. Considering their scattered regions of terrain and variety of land uses, urban outer edge have lesser landscape ordering and more turbulence. The physical measure known as information entropy highlights the unsteady land use status and disordered topography seen in metropolitan settings by quantifying the complexity and equilibrium of an ecosystem.

$$X = -\sum_{m=1}^{M} W_m Km(W_m) \qquad (17)$$

Where X is the landscape turbulence index (LTI), which is a helpful measure to assess the level of both the splitting and consistency of the terrain in each unit area. W_m is the proportion of a specific type of land in a single area to the total, and m is the number of different Regions corresponding to the land category in unit squares. The land cover data from 2011 and 2023were used to compute the LTI's significance over time $1000 \times 1000m$ unit grid that served as the model for the spatial LTI unit. After that, LTI was population- and GDP-adjusted, and it was interpolated with a 250-meter resolution using the Kriging technique.

The SVM is characterized as a unique ML algorithm that provides optimal solutions for issues such as over-fitting and local optimum. The SVM model is useful for several tasks, including pattern recognition and regression analysis. An expanded version of the conventional SVM model is used to translate a Quadratic Programming (QP) problem into linear equations. Effective in high-dimensional situations, the approach works even when there are more dimensions than samples. In this work, we are employing the SVM Classifier's unique design to categorize assaults. The vector input signal (x) is present in the input layer. In the hidden layer(y), it is calculated between the vector of the input signal (x) and the assistance vector(s). The linear outputs O of the buried layer neurons are added together by the output neuron. The detection of Distributed Denial-of-Service (DDoS) attacks is similar to the two classification problems; capitalize on the SVM algorithm's advantages, collect switch information to get training characteristic values, determine the effective hyperplane for categorization between the data from regular and DDoSattacks, and then acquire the classification results by validating our model using the test data, as following Equation (18).

$$O = \sum W_i k(x_i s_i) \qquad (18)$$

The hyperplane, also known as the decision function, is the foundation of the SVM for unbalanced binary categorization issues. It is described as Equation (19),

$$z(y) = u^D y + p = 0 \qquad (19)$$

With bias $p\epsilon K$ and weighted vector $u\epsilon K^M$. The following represents the constrained issue of an SVM having a maximum margin hyperplane Equation (20):

$$\min_{u,p,\beta_-,\beta_+} \frac{1}{2}\|u\|^2 + b_-\beta_- + b_+\beta_+ s.t. Y_-u + b_-p \le b_- - \beta_- Y_+u + b_+p \le v_+ - \beta_+\beta_- \ge 0 \qquad (20)$$

Where the maximal margins of two parallel hyperplanes are represented by the regularization term$\frac{1}{2}\|u\|^2$, the penalty parameters for controlling the weights between components for the positive and negative classes are b_+ andb_-, respectively. Slack variables for the negative classes and the positive class are $\beta-$ and $\beta+$. The training matrix for the negative classes and positive class are denoted by Y_- andY_+, and the vectors used for the negative classes and the positive class are, respectively, b_- andb_+.

RESULTS

Spatial-temporal dynamics of NP: The data shows that Guangzhou's average NP reduced from 807.45 $gC \cdot MJ \cdot m^{-2}$ in 2011 to 719.84 $gC \cdot m^{-2}$ in 2023. An uneven spatial arrangement was created as a result of the mean NP declining significantly from the northeast to the south due to various human disturbances and significant changes in land cover. There was also noticeable regional variability in this drop. The yearly mean NP values for each grid cell varied, with the northeast having more than 1189 $gC \cdot MJ \cdot m^{-2}$ and the middle section, which was primarily made up of built-up territory with little green areas, having 7$gC \cdot MJ \cdot m^{-2}$, It was mostly covered in woodlands shows in **Figure 2**.

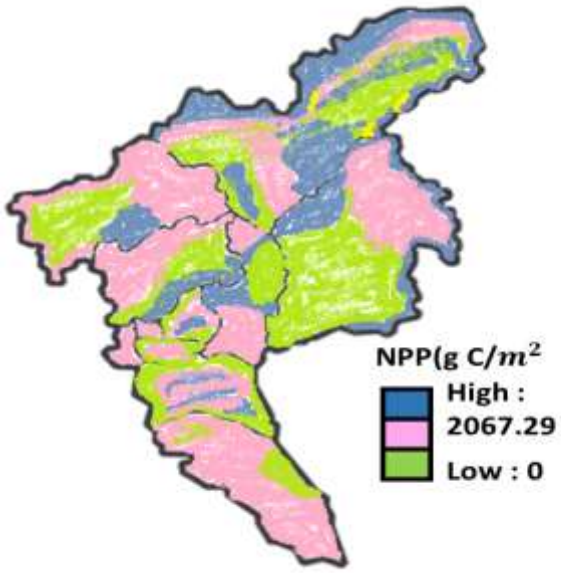

Figure 2. Spatial pattern of mean NP.

With an average slope of -10.94, more than 70% of Guangzhou's total pixels have seen a fall in NP during the last 13 years. This reduction is especially apparent in core regions. Only 3.44 percent of the total number of pixels showed evidence of a discernible upward movement,compared to 19.34% with a significant falling trend in **Figure 3.**

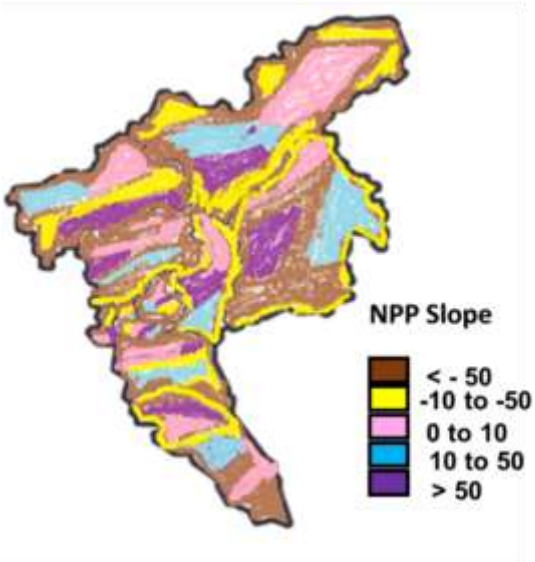

Figure 3. Modification in NPdevelopment.

Because of less human involvement and more stringent policy protection measures, the northeastern region's wooded areas had around 61.01% of the pixels with significant positive trends. Nonetheless, it is impossible to overlook the growing number of pixels with a decreasing tendency in **Figure 4.**

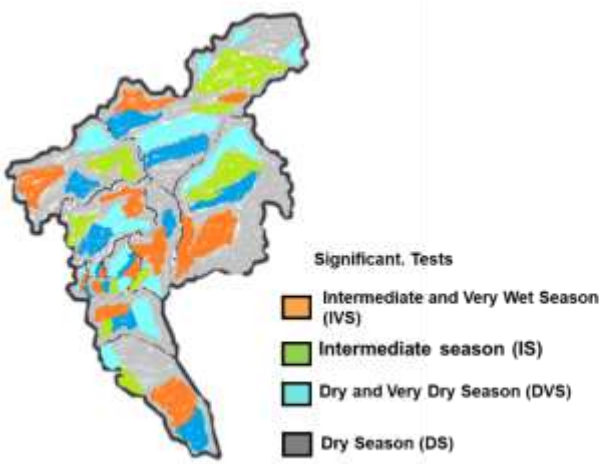

Figure 4. Significance Tests of spatial patterns and NP development.

Urban Growth's Spatial Patterns: Guangzhou has rapidly become an industrialized and urbanized city since 1978; this development continued and picked up speed between 2011 and 2023. Urban expansion and a reduction in other kinds of coverage of land resulted from increased demand for land for residential, commercial and industrial development due to factors such as labor shifts, population expansion, and economic development. Between 2011 and 2023, established land area decreased by 584.85 and 243.14 km², respectively, while urbanized and constructed lands grew to 979.72 km² at an 8.13% yearly pace.The largest area affected was crops, which had 320.93 km² turned into building land. The related frequency distributions for the geographic UDI values in 2011 (a) and 2023(b) are displayed in **Figure 5**.

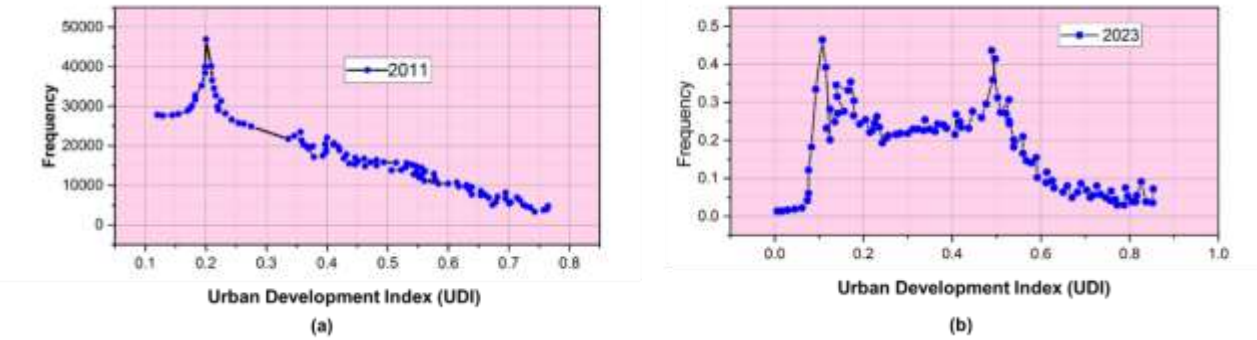

Figure 5. Corresponding frequency distributions for the spatial UDI values in 2011 (a) and 2023 (b).

Urbanization increased between 2011 and 2023, as evidenced by the mean UDI rising sharply from 0.1293 in 2011 to 0.2879 in 2023. With high values in metropolitan regions and low values outside of centers, UDI showed evident variety. Guangzhou City's urban geographic kinds were divided into three categories: exurb, fringe, and core. In 2011, the predominant geographic category was urban exurbs, accounting for up to 91.8% of the total area. Urban centers were concentrated in around Yuexiu, making up the smallest share (only 1.0%). Urban exurb regions dropped, whereas urban fringes grew surrounding previously identified areas along major routes to Guangzhou's north, northeast, and south.Guangzhou's vegetation growth was probably higher than that of the rest of Guangdong Province and the nation because of its larger vegetation covering and better hydrothermal conditions. By comparing the NPestimates from the MODIS NP Product with 403 randomly selected sample points against urban coresthe study was able to validate the NP estimations from the CASA model. The MOD17A3 data and our simulated findings showed a high agreement, through a correspondence value of 0.79 and a mean error of 15.07%. However, differences regarding MODIS instruments' and weather

data's spatial resolution, as well as changes in the model structure, parameters, and input data can introduce some errors in the NP predictions.

CONCLUSION

The consequences of urbanization on the environment have attracted a lot of attention on a local, provincial and universal scale. A deeper comprehension of trends in growth in cities and the ensuing spatial changes impact urban ecosystems is necessary for sustainable growth in cities. We examined NP trends in Guangzhou City between 2011 and 2023, measured NP as a measure of ecosystem services, and examined the impacts of urban developments on NP between 2011 and 2023 using the UDI, andSVM-based analytic tool. From 2011 to 2023, Guangzhou City experienced a decreasing trend in the average Park Preserved Area; while Urban Core Areas increased growing populations and financial growth were the causes of NP reductions and urban land expansion. A strong negative correlation was found between UDI and NP, indicating UDIwas a key factor influencing NP accumulation. NPwas considerable modifications and outer development as a result of repeated transitions between metropolitan cores, tresses, and exurbs.

REFERENCES

Ou, Y., Bao, Z., Ng, S. T., Song, W., & Chen, K. (2024). Land-use carbon emissions and built environment characteristics: A city-level quantitative analysis in emerging economies. Land Use Policy, 137, 107019.https://doi.org/10.1016/j.landusepol.2023.107019

Cheng, Z., Li, X., & Zhang, Q. (2023). Can new-type urbanization promote the green-intensive use of land? Journal of Environmental Management, 342, 118150.https://doi.org/10.1016/j.jenvman.2023.118150

Hou, Xianhui, et al. "Does economic agglomeration affect the sustainable intensification of cultivated land use? Evidence from China." Ecological Indicators 154 (2023): 110808.https://doi.org/10.1016/j.ecolind.2023.110808

Nuppenau, E. A. (2023). Contribution of peri-urban land use and agriculture to entropy and food of mega-cities: On sustainability, planning by control theory and recycling of organics. Plos one, 18(8), e0290747.https://doi.org/10.1371/journal.pone.0290747

Farooq, A., Farooq, N., Akbar, H., Hassan, Z. U., &Gheewala, S. H. (2023). A critical review of climate change impact at a global scale on cereal crop production. Agronomy, 13(1), 162.https://doi.org/10.3390/agronomy13010162

AbdelJawad, N., & Nagy, I. (2023). The Impacts of Urban Sprawl on Environmental Pollution, Agriculture, and Energy Consumption: Evidence From Amman City. Revista De Gestão Social E Ambiental, 17(2), e03347-e03347.https://doi.org/10.24857

Khan, T. I., Akbar, A., Jam, F. A., & Saeed, M. M. (2016). A time-lagged study of the relationship between big five personality and ethical ideology. Ethics & Behavior, 26(6), 488-506.

Jiao, L., Wu, Y., Fang, K., & Liu, X. (2023). Typo-Morphological Approaches for Maintaining the Sustainability of Local Traditional Culture: A Case Study of the Damazhan and Xiaomazhan Historical Area in Guangzhou. Buildings, 13(9), 2351.https://doi.org/10.3390/buildings13092351

Jam, F. A., Singh, S. K. G., Ng, B., & Aziz, N. (2018). The interactive effect of uncertainty avoidance cultural values and leadership styles on open service innovation: A look at malaysian healthcare sector. International Journal of Business and Administrative Studies, 4(5), 208-223.

Ye, C., Chen, W., Liu, Y., & He, Q. (2024). Institutionalization of public participation in China's urban regeneration from the perspective of historical institutionalism: Three-stage cases in Guangzhou. Political Geography, 108, 103036.https://doi.org/10.1016/j.polgeo.2023.103036

Liu, Y., Zhang, Y., Zhang, X., Han, F., & Zhao, Y. (2023). A geographical perspective on the formation of urban nightlife landscape. Humanities and Social Sciences Communications, 10(1), 1-15.https://doi.org/10.1057/s41599-023-01964-9

Ahmad, F., Shah, Z., & Al-Fagih, L. (2023). Applications of evolutionary game theory in urban road transport network: A state of the art review. Sustainable Cities and Society, 104791.https://doi.org/10.1016/j.scs.2023.104791

Jam, F. A., Singh, S. K. G., Ng, B., & Aziz, N. (2016). Interactive effects of Gender and Leadership Styles on Open Service Innovation: A Study of Malaysian Doctors, International Journal of Economics Research, 13(3), 1287-1304.

Liang, X., Zhao, T., &Biljecki, F. (2023). Revealing spatio-temporal evolution of urban visual environments with street view imagery. Landscape and Urban Planning, 237, 104802.https://doi.org/10.1016/j.landurbplan.2023.104802

Teo, S. S., Chung, C. K. L., & Wang, Z. (2023). Theorizing with urban China: Methodological and tactical experiments for a more global urban studies. Dialogues in Human Geography, 20438206231156656.https://doi.org/10.1177/20438206231156656

Liu, Y., Ma, C., & Huang, Z. (2023). Can the digital economy improve green total factor productivity? An empirical study based on Chinese urban data. Math. Biosci. Eng, 20(4), 6866-6893.https://doi.org/10.3934/mbe.2023296

Ke, Y., Liu, W., Wang, J., & Liu, F. (2023). How to promote the sustainable development of strategic emerging industries: Evidence from Guangzhou. Journal of Cleaner Production, 428, 139522.https://doi.org/10.1016/j.jclepro.2023.139522

Liu, C., Chen, J., &Xue, D. (2023). Daily mobilities with smartphone apps and their failures: A study in urban Guangzhou. Cities, 143, 104574.https://doi.org/10.1016/j.cities.2023.104574

Son, T. H., Weedon, Z., Yigitcanlar, T., Sanchez, T., Corchado, J. M., &Mehmood, R. (2023). Algorithmic urban planning for smart and sustainable development: Systematic review of the literature. Sustainable Cities and Society, 104562.https://doi.org/10.1016/j.scs.2023.104562

Henderson, K., &Loreau, M. (2023). A model of Sustainable Development Goals: Challenges and opportunities in promoting human well-being and environmental sustainability. Ecological modeling, 475, 110164. https://doi.org/10.1016/j.ecolmodel.2022.110164

Bibri, S. E. (2023). Data-driven smart eco-cities of the future: an empirically informed integrated model for strategic sustainable urban development. World Futures, 79(7-8), 703-746.https://doi.org/10.1080/02604027.2021.1969877